**Combining the highest degradation efficiency with the lowest environmental impact in zinc oxide based photocatalytic systems**

# Combining the highest degradation efficiency with the lowest environmental impact in ZnO-based catalytic systems

**M. Costamagna[a], L. Ciacci [b], M.C. Paganini, P. Calza[a], F. Passarini[b]**

[a] Department of Chemistry, University of Turin, Via P. Giuria 7-10125 Torino-Italy
[b] Department of Industrial Chemistry "Toso Montanari", University of Bologna, viale del Risorgimento 4, 40126 Bologna, Italy

## Abstract

In the present study we perform a comprehensive study of the photocatalytic abatement of a probe pollutant (phenol) in water in the presence of different photocatalysts by assessing the environmental impact associated to the~~i~~s specific process. We tested the performance of several ZnO-based materials doped with rare earth element (Ce, Er and Yb). An additional study parameter was the choice of the precursor of the dopant. Both rare-earth salts derived from chloride and nitrate were tested. -The experimental design allowed to define the two variables that greatly affect the process efficiency~~:, recognized as~~ the percentage of dopant and the concentration of photocatalyst. The life cycle assessment (LCA) methodology permits to evaluate the sustainability of the process and to identify some photocatalysts able to combine a high degradation efficiency with the minimization of the environmental impact.

Overall, the results identified cerium-doped ZnO as the most promising photocatalytic system, but univocal preference combining the fastest photodegradation with the lowest energy requirements and greenhouse gas (GHG) emission could not be assigned. The kinetic of degradation and environmental impacts resulted in two best operating ranges. When time to complete phenol degradation is priority, working with ZnO photocatalyst at a concentration of 1700 $mgL^{-1}$ and doped with Ce (1%) from nitrate precursor should be preferred. Instead, ZnO doped with Ce from chloride precursor (1%) enables to reduce energy requirements and material inputs as the optimal environmental profile occurs at a photocatalyst concentration between 800 and 1500 $mgL^{-1}$.

**Keywords**: zinc oxide, rare earth elements, LCA, experimental design

## 1. Introduction

The resources consumption, combined with the impact of human activities on the environment, has recently assumed a great relevance and, nowadays, sustainability is becoming a key aspect to be considered when evaluating a new process. Research is underway to find ways of augmenting water resources and water treatment and reuse is at the forefront of these technologies, so focusing on one side on the recycle and reuse of natural resources and materials aimed to prevent waste, and, on the other side, on the improvement of the remediation techniques. The incorporation of environmentally friendly techniques within the water treatment process is also, potentially, very lucrative.

Within this framework, heterogeneous photocatalysis has the great potential to be a cost-effective water purification technology for the removal of low concentration recalcitrant organic pollutants. Among the semiconductor oxides, titanium dioxide and zinc oxide seem to be the most promising candidates [1]. In previous papers, pure and Cerium (Ce) doped ZnO have been prepared *via* hydrothermal process, a low temperature, green and simple process to obtain controlled nanostructures, starting from different precursors. The synthesized materials permitted to achieve a fast degradation of phenol and several refractory compounds in ultrapure water at natural pH and under UV-Vis light conditions [2,3]. In a subsequent studies the investigation was extended to other dopants from rare earth elements (REEs), namely lanthanum (La), praseodymium (Pr), erbium (Er) and ytterbium (Yb). [2,3,4,5]

Thanks to their physical and chemical properties REEs are becoming increasingly important in several hi-tech applications such as clean energy technologies, hybrid vehicles, pollution control, optics, and refrigeration to name a few example[6]. However, an interconnected mine extraction route and imbalances between production and demand might cause future supply disruption for some REEs (e.g., neodymium and dysprosium) or oversupply and consequent material stockpiling for other REEs (e.g., lanthanum and cerium) with a cascade effect in their market price. Moreover, the production of REEs is far from being environmentally sustainable as it requires considerable inputs of materials and energy, and it generates large quantities of emissions and solid waste as well[7]. Therefore, analytical tools and strategies aiming at optimizing the use of REEs in common applications would result in the combined effect of increasing functionality while minimizing the associated environmental implications.

Following preliminary results, in the present paper we have evaluated and compared the process of the abatement of phenol in water by using different photocatalysts based on ZnO and doped with Ce, Er and Yb. Design of experiments (DoE) enables to explore and set the optimal experimental conditions with a relatively small number of experiments. Compared to traditional one-variable-at-time (OVAT) approach, DoE can extend the investigated domain to the interactions among experimental variables, which would be otherwise out of the reach with the conventional OVAT approach. The kinetic results of phenol photodegradation determined by DoE were then combined to life cycle assessment (LCA) methodology to quantify energy requirements and greenhouse gas (GHG) emissions associated with a photodegradation reaction of phenol in presence of ZnO-based photocatalysts to the ultimate goal of finding the catalytic system(s) that combines the highest degradation efficiency at the lowest environmental cost.

## 2. Materials and methods

### *2.1 Experimental design*

A DoE approach was followed to investigate the photocatalytic degradation of phenol in water solution from a set of ZnO photocatalysts doped with Ce, Er, and Yb. Overall, the photocatalytic reaction may depend on several operating parameters such as phenol concentration, concentration of the photocatalyst, type and

concentration of dopant elements, pH of water solution, size, structure, and surface area of the photocatalyst, reaction temperature, presence of inorganic ions, presence of oxygen, wavelength and irradiation time [8,9,10]. However, as dictated by the results obtained in previous studies[2,3,4,5] and by experience of the practitioners, the type and concentration of dopant in the photocatalyst ($X_1$) and the concentration of the catalytic system in solution ($X_2$) were set as the only factors of interest in DoE.

A faced centered design (FCD) model was utilised to determine linear and quadratic effect of $X_1$ and $X_2$ as well as interactions between $X_1$ and $X_2$. In FCD, a full factorial, a star design, and N replicates of the center pointes are modeled. Three levels (–1, 0, +1) were set for each variable (Table 1) based on concentration ranges derived from previous experiments. The three REEs (i.e., Ce, Er, and Yb) used as dopants of ZnO are treated as qualitative variables in FCD. Thus, the total number of experiments (N) for each doping element is computed as follows:

$$N = 2^f + 2f + N_0 \quad (1)$$

Where f is the number of variables and $N_0$ is the number of replicates in the centre points. Setting f = 2 and N = 2 respectively, the total number of experiments is 20 or 10 for each precursor (i.e., chloride and nitrate). However, the subset of experiments for $X_1$ at level –1, which correspond to bare ZnO photocatalyst, is common to both precursors. Thus, for each REEs investigated, the resulting total number of independent experiments reduced to 17 with two replicates of experiments in the center.

The mathematical model resulting from the FCD is in the form:

$$Y = B_0 + B_1X_1 + B_2X_2 + B_{11}X_{12} + B_{22}X_{22} + B_{12}X_1X_2 \quad (2)$$

Where Y is the calculated response, $X_1$ is the dopant concentration in the photocatalyst, $X_2$ is the concentration of the catalytic system employed in the photocatalytic degradation process. $B_0$ is the constant, $B_1$ is the coefficient of the linear effect of $X_1$, $B_2$ is the coefficient of the linear effect of $X_2$, $B_{11}$ is the coefficient of the quadratic effect of $X_1$, $B_{22}$ is the coefficient of the quadratic effect of $X_2$, $B_{12}$ is the coefficient of the interaction effect between $X_1$ and $X_2$.

| Variable | | | Level | | |
|---|---|---|---|---|---|
| # | **Description** | **Unit** | **–1** | **0** | **+1** |
| **$X_1$** | Rare earth element concentration | % w/w | 0 | 0.5 | 1 |
| **$X_2$** | Photocatalyst concentration | $mgL^{-1}$ | 100 | 800 | 1500 |

**Table 1.** Variables, investigated levels and their actual values utilised in the design of experiments.

According to the main goal of the study, the reaction rate constant k was the calculated response in all the experiments. The experiments were randomized to avoid external influence on the results and elaborated with a chemometric software developed by the Group of Chemometrics of the Italian Chemical Society in R (insert citation). The full experimental matrix for the FCD model created is reported in the Supporting Information (Table S1).

### *2.2 Experimental section*

$H_3PO_4$ (85%) was purchased from Carlo Erba. All the other reactants were purchased from Sigma-Aldrich with purity higher than 99.9% and were used without any further purification. HPLC grade water was obtained from MilliQ System Academic (Waters, Millipore).

Bare ZnO sample was synthesized starting from a 1 M water solution of $Zn(NO_3)_2 \cdot 6H_2O$. Then, a 4 M NaOH solution was added dropwise until the pH was 10-11. The solution was transferred into a 100 mL PTFE lined stainless steel autoclave (filling 70%) and then treated at 175°C overnight. The product was centrifuged, washed with deionized water, and dried at 70°C. The ZnO samples doped with rare earth elements (REEs) 1% molar were prepared by adding stoichiometric amounts of REEs in the starting solution. After that, the same procedure described above was followed; the path of synthesis has been taken from [2]. The precursor salts employed were respectively $CeCl_3 \cdot 7H_2O$ and $Ce(NO_3)_3 \cdot 6H_2O$ for cerium, $ErCl_3 \cdot 6H_2O$ and $Er(NO_3)_3 \cdot 5H_2O$ for erbium, $YbCl_3 \cdot 6H_2O$ and $Yb(NO_3)_3 \cdot 5H_2O$ for ytterbium. The samples were labelled as YZp-S where Y = dopant element (i.e., REE); Z = Zinc oxide; p = percentage of dopant in the photocatalysts (i.e, 0, 0.5, 1); S = type of salt used for as dopant precursor (i.e., Cl or $NO_3$).

The photocatalytic degradation performance of all synthesized photocatalysts was assessed using 60 $mgL^{-1}$ of phenol as a probe molecule. Samples irradiation was carried out using cylindrical Pyrex cells (4.0 cm diameter and 2.5 cm height, cut-off at 295 nm) filled with 5 mL of an aqueous suspension containing the phenol and the photocatalyst powder at the selected concentration. Samples were subjected to different irradiation times (ranging from 5 min to 3 h), using a set of six Actinic BL TL-D 15W (Phillips, Eindhoven, Nederland), the spectral region extends from 340 to 410 nm, with a maximum centred at 370 nm and a narrow band centred at 435 nm. The UV integrated irradiance on the cells in the 290–400 nm range wavelengths was 35 ± 1 $Wm^{-2}$ (lamps emission spectra and incident irradiance were recorded with a calibrated spectrum radiometer (Ocean Optics SD2000 CCD spectrophotometer, equipped with an optic fiber and a cosine corrector CC-3-UV-T)). During irradiation the suspensions were magnetically stirred.

After irradiation the suspensions were filtered through a 0.45 μm hydrophilic PTFE membrane (Millipore Millex-LCR). All samples were analysed by using a Merck-Hitachi liquid chromatographer equipped with a Rheodyne injector L-6200 and L-6200A pumps for high-pressure gradients, a L-4200 UV-Vis detector (the detection wavelength was set at 220 nm) and a column LiChrocart RP-C18 (Merck, 12,5 cm x 0,4 cm). Elution was carried out at 1 mL $min^{-1}$ with 4.2 mM aqueous $H_3PO_4$:$CH_3CN$ 70:30 in isocratic mode. The injection volume was 50 μL.

### *2.3 Assessment of environmental impacts*

LCA enables the assessment of the environmental impacts potentially caused by a product, a process or a service along its entire life cycle. According to ISO 14040 and 14044 the LCA methodology consists of four conceptual phases: goal and scope definition, life cycle inventory (LCI), life cycle impact assessment (LCIA), and results interpretation 11.

The goal and scope definition is the first step of a LCA analysis, and defines the object of the study, the system boundaries and the functional unit for all the flows. As earlier mentioned, the aim of this study is to evaluate and compare the efficiency of different photocatalysts that can be used for the degradation of organic pollutants in water. The term efficiency incorporates the sum of effectiveness, relative to the degradation behaviour, and low environmental impact of the materials. All the steps for the preparation of the photocatalysts and the phases of the degradation process have been included in the system boundary. Infrastructure and equipment used during the experimental analysis were instead excluded from calculation as well as the transport of input materials because their impact is expected to be marginal. The functional unit was set as the speed to complete degradation of 60 $mgL^{-1}$ of phenol in MilliQ water and measured as the reaction rate constant k expressed in $min^{-1}$.

An inventory of inputs and outputs was compiled with the intent to create a representative model of the system under scrutiny. Data acquisition of material and energy flows for rare earth oxide (REO) production,

synthesis of the precursors, synthesis of the photocatalysts and reaction of photodegradation was carried out from direct measurements in the laboratory and the existing literature. More in detail, REEs extraction is mainly carried out in China[12], via either open-pit mining of bastnäsite and monazite minerals or leaching of ion-adsorption clays. The Ecoinvent process "*Rare earth concentrate, 70% REO, from bastnäsite, at beneficiation*" provided the initial dataset to typical bastnäsite mining and refining in China[13]. Nuss and Eckelman[14] updated the Ecoinvent data by re-allocating energy/materials inputs and emissions based on Bayan Obo bastnäsite composition provided in Chinese Rare-Earth Year book 2010 and 2006–2010 REO prices. It is worth noting that the bastnäsite mineral usually contains about 50% of Cerium and only traces of the other two elements used as dopant in this study (Er and Yb). These two elements are part of the so-called group of heavy rare earth elements (HREEs). The production of HREEs (Tb, Dy, Ho, Er, Tm, Yb, and Lu) is mainly obtained from ion absorption deposits[15] and this pathway of recovery has not been investigated by Nuss and Eckelmann. More integrative research in this sense is needed.

As a process that models the energy production, used both during the synthesis phase and during the degradation phase, the Italian electric mix "Electricity, low voltage {IT}" was used.
Other assumptions made to conduct this LCA study are related to the synthesis of the precursors.
The data for zinc nitrate hexahydrate preparation was obtain from a patent [16]. For the cerium precursor the modelling was based for the chloride salts on "Synthetic Inorganic Chemistry" [17], and for the nitrate salt on "Preparation of rare earth nitrates" [18]. Since not all information has been found in literature, for some reactions the amount of water, energy and yield has been estimated, based on similar reactions; this is the case of the preparation of erbium and ytterbium nitrates, for which it was decided to model the synthesis in a similar way to the reaction of zinc nitrate; the only difference is the concentration of nitric acid that was obtained from the "Handbook of Chemistry and Physics" [19]. The inventory for the preparation of erbium chloride has been modelled based on the work of Gupta and Krishnamurthy [20] and the data for ytterbium chloride has been obtained from the paper of Sebastian and Seifert[21].
All the primary data, collected for the synthesis reactions of the photocatalysts and for the photodegradation process, refer to the laboratory scale.

The life cycle impact assessment was conducted with software SimaPro 8 and for selected indicators, namely: a) Cumulative Energy Demand (CED), which accounts for gross energy requirements[22], and b) Global Warming Potential IPCC 2013 GWP 100y, which is a metric for estimating the relative global warming contribution due to atmospheric emission of a kg of a particular greenhouse gas (GHG) compared to the emission of a kg of carbon dioxide[23] over a time horizon of 100 years.

Lastly, the outcomes of the inventory and of the impact assessment were discussed (i.e., interpretation of the results phase) to identify flows and substances with the most significant impacts both from the synthesis process and the degradation step.

## 3. Results and discussion

### *3.1 Photocatalytic degradation of phenol*

The photocatalytic activity of bare and REEs–doped ZnO photocatalysts was tested using phenol as a probe molecule and the degradation rate (DR) as a calculated response; direct photolysis and adsorption in the dark scarcely contributed to phenol attenuation [5].

Table 2 shows the DoE results for the photocatalytic degradation reaction obtained from ZnO–based materials doped with Ce, Er, and Yb and synthesized using either chloride or nitrate precursors. Overall, the presence of the REE–based dopant results in faster degradation rates than those achievable by bare ZnO

photocatalyst. These findings are aligned with preliminary results, but the FCD outcomes enabled here to investigate the entire domain of responses.

While for Ce– and Er–doped photocatalysts the choice of precursor seems not to influence remarkably the degradation rate of phenol, for Yb–doped photocatalyst a preference is given to the nitrate salt precursor. In terms of the calculated response, the three REEs used as dopants in ZnO photocatalyst rank as follows: Ce > Yb > Er. For Ce–doped ZnO catalytic systems from nitrate precursor the relationship between DR and investigated variables at coded scores is described by the following model (eq. 3). Similar results were obtained for Er– and Yb–doped photocatalysts, the related models of which are reported in the Supporting Information.

$$DR = 0.0696 + 0.0168X_1 + 0.0412X_2 + 0.0135X_1^2 + 0.00536X_2^2 - 0.0136X_1X_2 \qquad \text{(eq.3)}$$

The adjusted $r^2$ and the standard deviation of the residuals resulted in 0.94 and 0.0092 respectively. Figure 1 shows the significance of coefficients (i.e., *: $p < 0.05$; **: $p < 0.01$; ***: $p < 0.001$) for Ce-doped ZnO photocatalyst. Both $X_1$ and $X_2$ have an effect on the photochemical degradation, but the model seems to attribute the greatest significance (marked with ***) to the concentration of the photocatalyst ($X_2$). The concentration of the doping REE ($X_1$) in ZnO has a smaller linear effect but, notably, a more significant quadratic effect (at 95% confidence) than $X_2$. This evidence is clearly visible from the curve response surfaces but it was not detectable from the kinetic.

As mentioned, the higher k values were observed at the maximum value of $X_2$ and $X_1$ (Table 2), with the degradation rate increasing along the diagonal of Figure X1 and meaning that the effect of the photocatalyst increases at relatively high dopant concentrations. Because the best calculated responses were observed at the maximum values of $X_2$ and $X_1$, we decided to extend the investigated domain by carrying out, respectively, one experiment at bare ZnO concentration of 2000 $mgL^{-1}$, and two experiments with CeZn1-Cl at 1700 $mgL^{-1}$ and 2000 $mgL^{-1}$.

The degradation curves obtained for phenol as a function of the irradiation time in ultrapure water when using bare and Ce-doped ZnO are plotted in Figure 3, while those obtained with the other photocatalysts are shown in Figures S4-S5-S6 in the Supplementary Information. Figure 3 (a) reports the degradation performed using bare ZnO at different concentrations, while panel (b) shows the degradation curves obtained using ZnO doped with 1% of Ce, synthetized from chloride salt. These supplemental tests showed an increase in the photochemical degradation rate at photocatalyst concentrations between 1500 $mgL^{-1}$ to 2000 $mgL^{-1}$, with a relative "optimum" result achieved at 1700 $mgL^{-1}$. At higher concentrations, the degradation rate decreased. Possible reasons for such a slowdown of phenol photodegradation rate are a detrimental effect of the photocatalyst due to back reactions 24 as well as adsorption of phenol on the catalytic material and/or saturation phenomena. Similar results occurred also with Er– and Yb–doped photocatalysts.

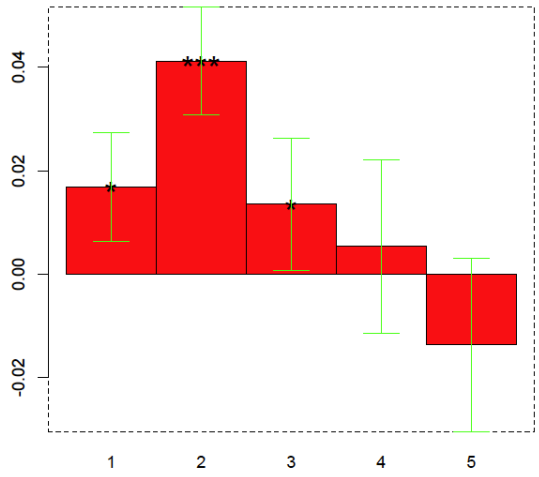


**Figure 1.** Estimation of the coefficients. Y-axis dimensionless.

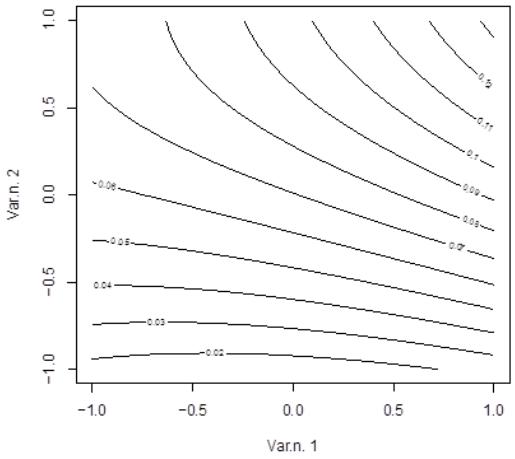


**Figure 2.** Response surface contour plot. Y-axis dimensionless.

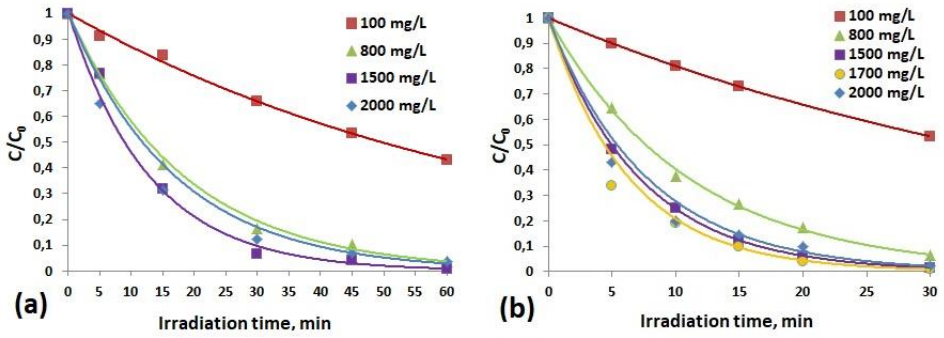


**Figure 3.** Reaction rate constant of phenol photodegradation at investigated concentrations of: (a) bare ZnO; and (b) ZnO doped with 1% of Cerium, synthesized from chloride salts CeZn1-Cl. $C/C_0$ indicates the ratio between the phenol concentration measured at a specific degradation time (C) and the initial concentration ($C_0$).

| k, $min^{-1}$ | Photocatalyst concentration, $mgL^{-1}$ | | | | |
|---|---|---|---|---|---|
| **Photocatalyst** | **100** | **800** | **1500** | **1700** | **2000** |
| **ZnO** | **0.014** | **0.055** | **0.078** | | **0.059** |
| **CeZn0.5-Cl** | **0.02** | **0.077** | **0.085** | | |
| **CeZn1-Cl** | **0.021** | **0.088** | **0.139** | **0.152** | **0.128** |
| **CeZn0.5-$NO_3$** | **0.012** | **0.074** | **0.109** | | |
| **CeZn1-$NO_3$** | **0.014** | **0.074** | **0.114** | **0.167** | |
| **ErZn0.5-Cl** | **0.011** | **0.061** | | | **0.091** |
| **ErZn1-Cl** | **0.013** | **0.062** | | **0.127** | **0.1** |
| **ErZn0.5-$NO_3$** | **0.012** | **0.048** | | | **0.081** |
| **ErZn1-$NO_3$** | **0.014** | **0.062** | | **0.124** | **0.111** |
| **YbZn0.5-Cl** | **0.013** | **0.061** | | | **0.086** |
| **YbZn1-Cl** | **0.012** | **0.06** | | **0.107** | **0.084** |
| **YbZn0.5-$NO_3$** | **0.011** | **0.062** | | | **0.109** |
| **YbZn1-$NO_3$** | **0.012** | **0.066** | | **0.114** | **0.109** |

**Table 2**. Rate constants (k, $min^{-1}$) of phenol degradation obtained in the presence of different photocatalysts as a function of photocatalyst concentration. The samples were labelled as YZp-S where Y = dopant element (i.e., REE); Z = Zinc oxide; p = percentage of dopant in the photocatalysts (i.e, 0, 0.5, 1); S = type of salt used for as dopant precursor (i.e., Cl or $NO_3$).

### *3.3 LCA for the photocatalytic process*

The investigation (evaluation) -about the consumed energy throughout the life cycle was assessed through the CED method and, as an example, Figure 4 shows LCIA results accounting for the production of 1.6939 g of CeZn1-Cl. The greatest energy requirement (i.e., about 98% of total CED) is associated to the electricity consumed during the sample treatment at 175°C overnight, followed by the energy required for the synthesis of ZnO from zinc nitrate and sodium hydroxide; conversely, the supply of the dopant is marginal. Similar

process contributions were also achieved for the other photocatalytic systems, with relatively small difference due to the production route of dopant precursors.

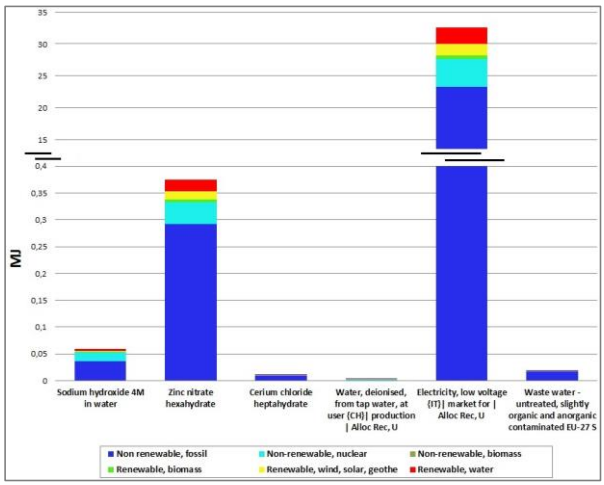


**Figure 4**. Cumulative Energy Demand (CED) of the synthesized photocatalyst: Ce-doped (1%) ZnO (CeZn1-Cl). Output of the synthesis is 1.6939 g of photocatalysts.

The effect of photocatalyst concentration on the energy requirement is explored in Figure 5, where CED results are computed as a function of CeZn1-Cl concentrations in the range 100-2000 $mgL^{-1}$. The complete degradation of 60 $mgL^{-1}$ of phenol in 5 ml of solution was selected as a functional unit for comparing the different results. When employing the photocatalyst at 100 $mgL^{-1}$, the complete photodegradation of phenol requires a protracted irradiation time and it results in the largest amount of energy inputs in the investigated domain. The system requires the lowest energy inputs when employing a concentration of 800 $mgL^{-1}$. Then, CED progressively increases at higher concentrations, but still remains lower than the energy inputs required at 100 $mgL^{-1}$. Absolute CED associated to electricity consumption remains almost constant from 1500 to 2000 $mgL^{-1}$, so suggesting that the lowest energy requirement ensues for photocatalyst concentration ≥ 1500 $mgL^{-1}$. On the other hand, the synthesis of the photocatalyst at intermediate (800 $mgL^{-1}$) to high (2000 $mgL^{-1}$) concentrations requires higher CED, both in absolute and relative (i.e., percent contribution) terms, contributing up to about 75% of total required energy.

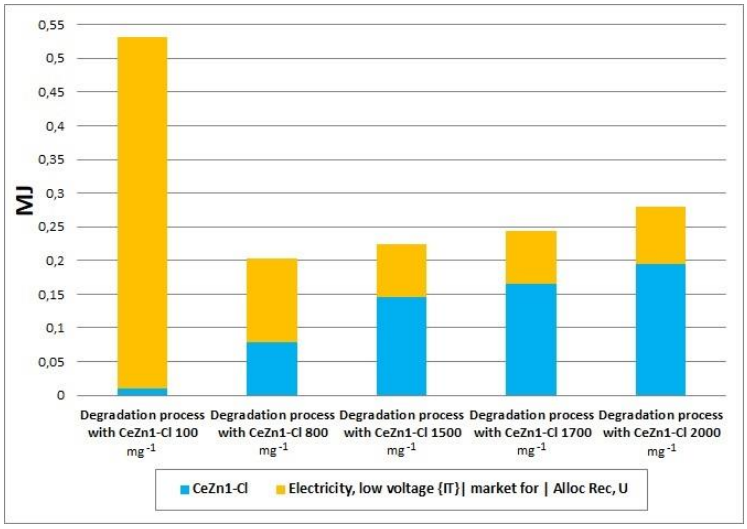


**Figure 5.** Comparison of the LCIA results for the degradation process using the Cumulative Energy Demand (MJ) method as a function of the photocatalyst concentration.

Table 3 summarises FCD results (on the top) and LCA findings (on the bottom) providing the basis for discussing the outcome of kinetics and environmental implications on phenol degradation. In both panels a heat map introduces a colour gradient that marks the results from red (the worst score) to green (the best score). Even if a combination of the fastest degradation rate with the lowest energy inputs is not achieved, the most promising outcome matches with Ce-doped (1%) ZnO, so setting the basis for the identification of the "best" working conditions.

In particular, the highest degradation rate was achieved with CeZn1-$NO_3$ at a concentration of 1700 $mgL^{-1}$, i.e. when employing the highest quantity of photocatalyst and dopant. The (relative) optimal working conditions could be established by reduction 12% of photocatalyst concentration (i.e. from 1700 $mgL^{-1}$ to 1500 $mgL^{-1}$) that results in 9% reduction on the degradation rate. Conversely, CED values assess that the lowest energy requirement occurs for CeZn1-Cl at 800 $mgL^{-1}$, while working at 1500 $mgL^{-1}$ and 1700 $mgL^{-1}$ concentrations produce an increase of 11% and 18%, respectively. Therefore, the optimal conditions for the degradation of phenol in water are achieved in presence of CeZn1-Cl in the range 800-1500 $mgL^{-1}$.

| | K, min$^{-1}$ | | | | |
|---|---|---|---|---|---|
| **photocatalyst** | **100 mgL$^{-1}$** | **800 mgL$^{-1}$** | **1500 mgL$^{-1}$** | **1700 mgL$^{-1}$** | **2000 mgL$^{-1}$** |
| **ZnO** | **0.014** | **0.055** | **0.078** | | **0.059** |
| **CeZn0.5- Cl** | **0.02** | **0.077** | **0.085** | | |
| **CeZn1-Cl** | **0.021** | **0.088** | **0.139** | **0.152** | **0.128** |
| **CeZn0.5-$NO_3$** | **0.012** | **0.074** | **0.109** | | |
| **CeZn1-$NO_3$** | **0.014** | **0.074** | **0.114** | **0.167** | |
| **ErZn0.5-Cl** | **0.011** | **0.061** | | | **0.091** |
| **ErZn1-Cl** | **0.013** | **0.062** | | **0.127** | **0.1** |
| **ErZn0.5-$NO_3$** | **0.012** | **0.048** | | | **0.081** |
| **ErZn1-$NO_3$** | **0.014** | **0.062** | | **0.124** | **0.111** |
| **YbZn0.5-Cl** | **0.013** | **0.061** | | | **0.086** |
| **YbZn1-Cl** | **0.012** | **0.06** | | **0.107** | **0.084** |
| **YbZn0.5-$NO_3$** | **0.011** | **0.062** | | | **0.109** |
| **YbZn1-$NO_3$** | **0.012** | **0.066** | | **0.114** | **0.109** |
| | | | | | |
| | **CED (MJ)** | | | | |
| **photocatalyst** | **100 mgL$^{-1}$** | **800 mgL$^{-1}$** | **1500 mgL$^{-1}$** | **1700 mgL$^{-1}$** | **2000 mgL$^{-1}$** |
| **ZnO** | **792** | **280** | **292** | | **388** |
| **CeZn0.5- Cl** | **557** | **222** | **278** | | |
| **CeZn1- Cl** | **531** | **202** | **225** | **238** | **280** |
| **CeZn0.5-$NO_3$** | **922** | **227** | **249** | | |
| **CeZn1-$NO_3$** | **792** | **226** | **242** | **231** | |
| **ErZn0.5-Cl** | **1010** | **259** | | | **318** |
| **ErZn1-Cl** | **852** | **254** | | **251** | **303** |
| **EZ0.5-H $NO_3$** | **922** | **307** | | | **333** |
| **ErZn1-$NO_3$** | **792** | **254** | | **253** | **292** |
| **YbZn0.5-Cl** | **852** | **259** | | | **326** |
| **YbZn1-Cl** | **922** | **260** | | **267** | **324** |
| **YbZn0.5-$NO_3$** | **1010** | **256** | | | **299** |
| **YbZn1-$NO_3$** | **922** | **243** | | **261** | **294** |

**Table 3.** Kinetic results from Faced Centered Design experiments (top) and associated life cycle impact assessment results for Cumulative Energy Demand (CED, bottom). The heat map introduces a colour gradient that differentiates the results from red (the worst score) to green (the best score).

The impact assessment was also performed using the Global Warming Potential IPCC 2013 (GWP) 100y, an index useful for estimating the relative global warming contribution associated with the release of greenhouse gases (GHG) and results are summarized in Table 4. LCIA analysis performed with the GWP method reflects the same trend already observed with the CED method. The synthesis process involves the release of 1.8856 kg $CO_2$ eq to produce 1.6939 g of CeZn1-Cl (Figure S4); the degradation processes performed with CeZn1-Cl as photocatalyst, at different concentrations, show the same emission trend of $CO_2$ equivalents with respect to the energy consumption obtained previously (Figure S5). ~~When w~~Working at the "best" operational conditions the reduction in electrical energy requirement to promote photodegradation of phenol would determine a minimum of GHG emissions to 11.5-13.2 g$CO_2$ eq.

Consequently, lower concentrations of Ce-doped ZnO ~~produced (~~from chloride precursor) may be preferable when the cost of electrical energy or of the catalytic materials is~~are~~ prevailing, while the fastest degradation rates are instead achievable at higher concentrations ~~and~~ in particular from nitrate precursor.

**Commentato [MCP1]:** Scusa l'ignoranza ma LCIA è volute o un refuse di LCA???

| | K, $min^{-1}$ | | | | |
|---|---|---|---|---|---|
| **photocatalyst** | **100 $mgL^{-1}$** | **800 $mgL^{-1}$** | **1500 $mgL^{-1}$** | **1700 $mgL^{-1}$** | **2000 $mgL^{-1}$** |
| **ZnO** | **0.014** | **0.055** | **0.078** | | **0.059** |
| **CeZn0.5- Cl** | **0.02** | **0.077** | **0.085** | | |
| **CeZn1-Cl** | **0.021** | **0.088** | **0.139** | **0.152** | **0.128** |
| **CeZn0.5-$NO_3$** | **0.012** | **0.074** | **0.109** | | |
| **CeZn1-$NO_3$** | **0.014** | **0.074** | **0.114** | **0.167** | |
| **ErZn0.5-Cl** | **0.011** | **0.061** | | | **0.091** |
| **ErZn1-Cl** | **0.013** | **0.062** | | **0.127** | **0.1** |
| **ErZn0.5-$NO_3$** | **0.012** | **0.048** | | | **0.081** |
| **ErZn1-$NO_3$** | **0.014** | **0.062** | | **0.124** | **0.111** |
| **YbZn0.5-Cl** | **0.013** | **0.061** | | | **0.086** |
| **YbZn1-Cl** | **0.012** | **0.06** | | **0.107** | **0.084** |
| **YbZn0.5-$NO_3$** | **0.011** | **0.062** | | | **0.109** |
| **YbZn1-$NO_3$** | **0.012** | **0.066** | | **0.114** | **0.109** |

| | GWP (g $CO_2$ eq) | | | | |
|---|---|---|---|---|---|
| **Photocatalyst** | **100 $mgL^{-1}$** | **800 $mgL^{-1}$** | **1500 $mgL^{-1}$** | **1700 $mgL^{-1}$** | **2000 $mgL^{-1}$** |
| **ZnO** | **45.0** | **15.9** | **16.7** | | **22.1** |
| **CeZn0.5- Cl** | **31.7** | **12.6** | **15.8** | | |
| **CeZn1-Cl** | **30.2** | **11.5** | **12.8** | **13.9** | **16.0** |
| **CeZn0.5-$NO_3$** | **52.4** | **12.9** | **14.2** | | |
| **CeZn1-$NO_3$** | **45.0** | **12.9** | **13.8** | **13.2** | |
| **ErZn0.5-Cl** | **57.1** | **14.7** | | | **18.2** |
| **ErZn1-Cl** | **48.4** | **14.5** | | **14.3** | **17.3** |
| **ErZn0.5-$NO_3$** | **52.4** | **17.5** | | | **19.0** |
| **ErZn1-$NO_3$** | **45.0** | **14.5** | | **14.4** | **16.7** |
| **YbZn0.5-Cl** | **48.4** | **14.7** | | | **18.6** |
| **YbZn1-Cl** | **52.4** | **14.8** | | **15.2** | **18.5** |
| **YbZn0.5-$NO_3$** | **57.1** | **14.6** | | | **17.0** |
| **YbZn1-$NO_3$** | **52.4** | **13.8** | | **14.9** | **16.8** |

**Table 4.** Kinetic results from Faced Centered Design experiments (table at the top) associated to life cycle impact assessment results for Global Warming Potential (GWP). The heat map introduces a colour gradient that differentiates the results from red (the worst score) to green (the best score).

## Conclusive remarks

The photocatalytic process represents an attractive route for the degradation of hazardous pollutants in water treatment and, for such, together with, it is also important not only the evaluation of the photodegradation performance of these processes/materials, but also to investigate the possible environmental burdens associated with them. In this work, we proved that an integrated application of DoE and LCA can enlighten the setting of operating conditions in water treatments for pollutants removal and environmental protection.

DoE enabled to model the photodegradation of phenol in water solution as a function of type, concentration and precursor route of REE used as a dopant in ZnO photocatalysts, and concentration of the catalytic system itself in water solution. LCA informed about the environmental impact outcomes for Cumulative Energy Demand and Global Warming Potential associated to the catalytic systems under scrutiny, setting the basis for achieving the greatest efficiency at the lowest environmental cost.

Results pointed out that even if highest degradation efficiency is obtained with 1700 $mgL^{-1}$ of ZnO doped with 1% of rare earth element, it is desirable to perform the degradation process using a lower photocatalyst concentration (around 800 $mgL^{-1}$) so containing the environmental impact.

Perspectives of future work could consider to perform the photodegradation in a real water matrix, aimed to assess whether the kinetic results and impacts associated with the degradation process reflect the results obtained in this study. A further improvement of the synthesized photocatalysts could be obtained if they could be easily recovered from the aqueous solution. A way to extend their lifetime and therefore reduce the impact associated with the production phase, could be to support these materials on fibres or membranes, so that they can be easily removed from the treated matrix.

**Acknowledgments**

We acknowledge support from a Marie Curie International Research Staff Exchange Scheme Fellowship (MAT4TREAT, proposal no. 645551) within the Horizon 2020 European Community Framework Programme.

**Supporting Information**. In the supporting information file, were reported both the significance of coefficients for all the REEs-doped ZnO from chloride and nitrate precursors both the response surface contour plot for all the photocatalysts. Also the degradation curves obtained for the degradation of the phenol were reported; the curves were grouped per type of element used as dopant.

The LCIA results, using the Global Warming Potential IPCC 2013 GWP 100y method, of the synthesis of CeZn1-Cl were also reported. As well as the comparison of the LCIA results for the degradation process using CeZn1-Cl at different concentration, results obtained using the IPCC 2013 GWP 100y method.

## References


1) Lee, K. M.; Lai, C. W.; Ngai, K. S.; Juan, J. C.; Recent developments of zinc oxide based photocatalyst in water treatment technology: A review. Water Research. 2015. http://dx.doi.org/10.1016/j.watres.2015.09.045.
2) Calza, P.; Gionco, C.; Giletta, M.; Kalaboka, M.; Sakkas, V. A.; Albanis, T.; Paganini, M. C. Assessment of the Abatement of Acelsulfame K Using Cerium Doped ZnO as Photocatalyst. J. Hazard. Mater. 2017. https://doi.org/10.1016/j.jhazmat.2016.03.093.
3) Paganini, M. C.; Dalmasso, D.; Gionco, C.; Polliotto, V.; Mantilleri, L.; Calza, P. Beyond TiO2: Cerium-Doped Zinc Oxide as a New Photocatalyst for the Photodegradation of Persistent Pollutants. ChemistrySelect 2016, 1 (12), 3377–3383. https://doi.org/10.1002/slct.201600645.
4) Cerrato, E.; Gionco, C.; Berruti, I.; Sordello, F.; Calza, P.; Paganini, M. C. Rare Earth Ions Doped ZnO: Synthesis, Characterization and Preliminary Photoactivity Assessment. J. Solid State Chem. 2018, 264 (April), 42–47. https://doi.org/10.1016/j.jssc.2018.05.001.
5) Sordello, F.; Berruti, I.; Gionco, C.; Paganini, M. C.; Calza, P.; Minero, C. Photocatalytic Performances of Rare Earth Element-Doped Zinc Oxide toward Pollutant Abatement in Water and Wastewater. Appl. Catal. B Environ. 2019, 245 (September 2018), 159–166. https://doi.org/S0926337318312062.
6) Koltun, P.; Tharumarajah, A. Life Cycle Impact of Rare Earth Elements. ISRN Metall. 2014. https://doi.org/10.1155/2014/907536.
7) Navarro, J.; Zhao, F. Life-Cycle Assessment of the Production of Rare-Earth Elements for Energy Applications: A Review. Front. Energy Res. 2014. https://doi.org/10.3389/fenrg.2014.00045.
8) Kumar, A. A Review on the Factors Affecting the Photocatalytic Degradation of Hazardous Materials. Mater. Sci. Eng. Int. J. 2017, 1 (3), 1–10. https://doi.org/10.15406/mseij.2017.01.00018.
9) Márquez, J. A. R.; Herrera, C. M.; Fuentes, M. L.; Rosas, L. M. Effect of Three Operating Variables on Degradation of Methylene Blue by ZnO Electrodeposited: Response Surface Methodology. Int. J. Electrochem. Sci. 2012, 7 (11), 11043–11051.
10) Reza, K. M.; Kurny, A.; Gulshan, F. Parameters Affecting the Photocatalytic Degradation of Dyes Using TiO2: A Review. Appl. Water Sci. 2017, 7 (4), 1569–1578. https://doi.org/10.1007/s13201-015-0367-y.
11) https://www.iso.org/standard/37456.html
12) Hellman, P. L.; Duncan, R. K. Evaluation of Rare Earth Element Deposits. Appl. Earth Sci. 2014. https://doi.org/10.1179/1743275814Y.0000000054.
13) H.-J., A.; Chudacoff, M.; Hischier, R.; Osses, M., A.; Primas, A. Life Cycle Inventories of Chemicals. Ecoinvent Report No.8, v2.0. Final Rep. ecoinvent data … 2007, No. 8, 1–957.
14) Nuss, P.; Eckelman, M. J. Life Cycle Assessment of Metals: A Scientific Synthesis. PLoS One 2014. https://doi.org/10.1371/journal.pone.0101298.
15) Talens Peiró, L.; Villalba Méndez, G. Material and Energy Requirement for Rare Earth Production. JOM 2013. https://doi.org/10.1007/s11837-013-0719-8.
16) August, M.; Process for preparing pulverulent hydrates of zinc nitrate, patent US3206281A.
17) Blanchard, Arthur A.; Phelan, Joseph W.; Davis, Arthur R.; Synthetic Inorganic Chemistry. Fifth edition. 286-287, 1936.
18) Pitts, F.; Preparation of rare earth nitrates, patent US4231997A.
19) John R. Rumble ; CRC Handbook of Chemistry and Physics, 99th Edition.
20) Gupta, C.K.; Krishnamurthy, N.; Extractive metallurgy of rare earth; pag 214; 2005
21) Sebastian, J.; Seifert, H.-J.; Ternary chlorides in the systems ACl/$YbCl_3$ (A=Cs,Rb,K); Thermochimica Acta 318(1998)29±37 https://doi.org/10.1016/S0040-6031(98)00326-8.

22) Frischknecht, R.; Editors, N. J.; Althaus, H.; Bauer, C.; Doka, G.; Dones, R.; Hischier, R.; Hellweg, S.; Köllner, T.; Loerincik, Y.; et al. Implementation of Life Cycle Impact Assessment Methods; 2007. https://doi.org/citeulike-article-id:4863951.
23) Houghton JT; Y, D.; DJ, G.; M, N.; PJ, van der L.; X, D.; K, M.; C, J. Climate Change 2001: The Scientific Basis; 2001. https://doi.org/10.1256/004316502320517344.
24) Minero, C.; Vione, D. A Quantitative Evalution of the Photocatalytic Performance of $TiO_2$ slurries. Appl. Catal. B Environ. 2006. https://doi.org/10.1016/j.apcatb.2006.05.011.